Ultrasonic equation of state of rhenium*

Murli H. Manghnani and Keith Katahara
Hawaii Institute of Geophysics, University of Hawaii, Honolulu, Hawaii 96822

Edward S. Fisher
Argonne National Laboratory, Argonne, Illinois 60439

(Received 23 April 1973)

The elastic constants C_{ij} of single-crystal Re and their pressure derivatives dC_{ii}/dP, measured to 4.2 kbar at 25 °C, are, respectively; C_{11}: 6177.3 and 8.65; C_{33}: 6828.2 and 8.45; C_{13}: 2055.7 and 2.98; C_{44}: 1605.4 and 1.49; C_{66}: 1714.1 and 1.56. The initial pressure derivative of the isothermal bulk modulus, $K_T' = (\partial K_T/\partial P)_{P=0}$, calculated from the Voigt-Reuss-Hill approximation, is 5.43, which is significantly larger than the previously reported value of 2.93 based on x-ray-diffraction data. The contributions to K_T and K_T' from long-range Fermi energy and short-range ion-core repulsive interactions (K_F and K_{SR}, respectively) are evaluated by assuming the Born-Mayer potentials for the latter contribution. Using an empirical relationship between atomic volume and K_T' ($\approx K_s'$), it is found that the x-ray value for K_T' is probably too low. Evaluation of the Born-Mayer parameters leads to the conclusion that the short-range contribution, rather than the Fermi contribution, dominates K_T, and shear moduli C_{44} and C_{66}, and their pressure derivatives, whereas the Fermi energy is a major contributory factor in the case of shear modulus $C_H = (1/6)(C_{11} + C_{12} + 2C_{33} - 4C_{13})$. The latter conclusion is strengthened by the nonlinearity of C_H with respect to pressure, and by the anomalous variation of the superconducting temperature T_c with pressure, which effect is related to the change in Fermi-surface topology. The value of the Grüneisen-mode gamma γ_H for Re, calculated from the dC_{ij}/dP, 1.83, which is significantly less than thermal gamma γ_{th} (2.39) at 300 °K.

I. INTRODUCTION

Rhenium, which crystallizes in hexagonal close-packed structure (hcp), has an axial c/a ratio of 1.615 at 25 °C, slightly less than the ideal value of 1.633. Among all the metals studied, it has the second-highest bulk-modulus value ($K_T = 3603$ kbar). Temperature dependence of the single-crystal elastic constants C_{ij} has been investigated for Re in the temperature range 4–923 °K.[1,2] Recently, Liu *et al.*,[3] employing x-ray-diffraction techniques, have determined the effects of pressure to 350 kbar and of temperature to 701 °K on the lattice parameters of rhenium. These authors, by analyzing their V/V_0 pressure data in light of the Birch-Murnaghan equation of state, have derived values of the isothermal bulk modulus K_T and its initial pressure derivative $K_T' = (\partial K_T/\partial P)_{P=0}$, as being equal to 3500 ± 150 kbar and 2.93 ± 1.33 kbar, respectively. Their value of K_T' seems rather low and would imply that the short-range ion-core repulsive contribution to the elastic constants and their volume derivatives is considerably smaller than indicated by the high value of K_T.

One of the most interesting findings in research on this metal is the anomalous (negative) pressure dependence of the superconducting transition temperature T_c, which Chu *et al.*[4] observed at low pressures. They found that T_c decreases with increasing pressure, reaching a minimum at about 7 kbar, and then increases with higher pressures before leveling off at 13–18 kbar. This anomalous effect has been related to change in the Fermi-surface topology with pressure, leading to a change in the density of electron energy states at the Fermi surface.[4,5]

In view of the above and a general interest in the effect of atomic volume on the various contributions to the C_{ij} and their pressure derivatives in hcp metals, we have investigated the elastic constants of single-crystal Re under hydrostatic pressure to 4.2 kbar. The purpose of this paper is threefold: (i) to ascertain K_T' directly from the ultrasonic measurements, and to use the value in the Birch-Murnaghan equation of state for evaluating V/V_0 as a function of pressure, so as to correlate the results with x-ray and shock-wave data[6]; (ii) to analyze the C_{ij} data in light of the electrostatic contributions to the shear elastic constants, and to interpret the pressure derivatives of the bulk modulus and shear elastic constants in terms of the short-range ion-core repulsive-force potentials in the Born-Mayer equation; and (iii) to determine whether the change in the Fermi-surface topology at low pressures, as indicated by the superconductivity measurements, is also reflected in the pressure dependence of the C_{ij} of Re.

II. EXPERIMENTAL PROCEDURES

The same two single-crystal specimens of Re employed in a previous study[2] were used in this investigation. The original crystal faces had to be repolished; hence the path lengths have changed slightly. X-ray back-reflection Laue patterns

TABLE I. Basic frequency and velocity data for Re at 25°C and 1 bar.

Crystal specimen No.	Direction of propagation	Direction of vibration	Mode	Mode No.	Length[a] (mm)	Pulse repetition frequency (kHz)	Velocity (km/sec)	Elastic coefficient determined
A	∥ to *a*	∥ to *a*	longitudinal	1	4.4888	603.786	5.4205	$\rho v_1^2 = C_{11}$
A	∥ to *c*	∥ to *c*	longitudinal	2	5.2667	541.042	5.6990	$\rho v_2^2 = C_{33}$
A	∥ to *c*	any	shear	3	5.2680	262.258	2.7631	$\rho v_3^2 = C_{44}$
A	∥ to *a*	∥ to *c*	shear	3*A*	4.5481	303.790	2.7633	$\rho v_{3A}^2 = C_{44A}$
A	∥ to *a*	∥ to *b*	shear	4	4.5491	313.831	2.8553	$\rho v_4^2 = C_{66} = \frac{1}{2}(C_{11} - C_{12})$
B	45° to *a* and *c*	45° to *a* and *c*	quasilongitudinal	5	4.6647	567.432	5.2919	$\rho v^2 = C_{RS}$[b]

[a]Different lengths appear because of relapping and repolishing of specimen faces.
[b]$C_{RS} = \{C_{11} + C_{33} + 2C_{44} + [(C_{11} - C_{33})^2 + 4(C_{13} + C_{44})^2]^{1/2}\}/4$.

were taken to provide rechecks on the orientation of the faces to within $\pm\frac{1}{2}°$ of the intended directions.

McSkimin's pulse-superposition (PSP) method,[7] employed in this study for the velocity measurements, is outlined in a previous paper.[8] The high-pressure equipment, also described previously,[9] consists of a Hardwood two-stage pressure-intensifying system, a high-pressure vessel with a constant-temperature bath, and a manganin cell in combination with a Carey-Foster pressure-measuring bridge, which was calibrated with a Harwood DWT-300 dead-weight tester. Nitrogen was used as the gas medium. *X*-cut and *Y*-cut quartz transducers, $\frac{1}{8}$-in. in diameter with 20-MHz natural resonant frequency, were used to generate waves in the specimens. Dow-Corning resin (276-*V*9) was used as a bond between specimen and transducer.

Crystal *A* with two sets of faces, perpendicular to the *a* and *c* crystallographic axes allowed measurements of C_{11}, C_{33}, C_{44}, and $C_{66} = \frac{1}{2}(C_{11} - C_{12})$. Good agreement between the two values of C_{44} and $C_{44\,A}$ (Table I), determined from wave velocities in two different directions, provided an additional check on the orientation of the crystal faces. The remaining elastic constant, C_{13}, was determined from the quasilongitudinal velocity in crystal *B* in the direction 45° to the *a* and *c* crystallographic axes (see Table I).

The basic pulse-repetition-frequency (prf) measurements were carried out at (25 ± 0.1) °C and 1 bar, and to ≈4.2 kbar, in increasing steps of 0.27 kbar. A time interval of at least 15 min was allowed between pressurization cycle and prf measurement.

III. EXPERIMENTAL DATA AND RESULTS

A. Single-crystal elastic constants

Table I lists the basic pulse-repetition frequency *f* and velocity data of Re at 25 °C and 1 bar, velocities having been computed from $v = 2fl$, where *l* is the path length in the crystal. In Table I, ρ is the density (21.024 g/cm^3, Ref. 2). Based on estimated experimental errors and adjudged accuracy of the PSP method, the velocity values are considered to be correct within ±0.05%. A comparison between the elastic-constant values for Re determined in this study and those obtained previously by the other investigators[1,2] is shown in Table II.

Fisher and Dever's[2] uncertainties in C_{ij} values are based on checks of internal consistency. Since the same crystals were used, our values are subject to the same uncertainties, plus perhaps another ±0.05% due to diffraction and geometrical effects, and to bond effects which were ignored in the present study.

The uncertainties in C_{12} and C_{13} values are greater than those for the other C_{ij} because the former are calculated and not directly measured. Except for the C_{44} value reported by Shepard and Smith, agreement between the present and earlier reported C_{ij} values is quite satisfactory.

Figure 1 is a plot of the ratio of prf at a given pressure to that at zero applied pressure (f_n/f_{n_0}) versus pressure to 4.2 kbar for the five different modes of propagation as explained in Table I. As

TABLE II. A comparison of the measurements of the elastic constants (in kbar) of Re with previous work (Refs. 1 and 2).

Elastic constant	Shepard and Smith (Ref. 1)	Fisher and Dever (Ref. 2)	This study
C_{11}	6126 ± 0.2%	6181.5 ± 0.15%	6177.3 ± 0.2%
C_{33}	6827 ± 0.2%	6835.0 ± 0.15%	6828.2 ± 0.2%
C_{44}	1625 ± 0.2%	1606.2 ± 0.15%	1605.4 ± 0.2%
C_{66}	1714 ± 0.2%	1714.4 ± 0.15%	1714.1 ± 0.2%
C_{12}	2700 ± 0.8%	2752.7 ± 0.15%	2749.1 ± 0.2%
C_{13}	2060 ± 1.3%	2041.7 ± 1–1.5%	2055.7 ± 1–1.5%

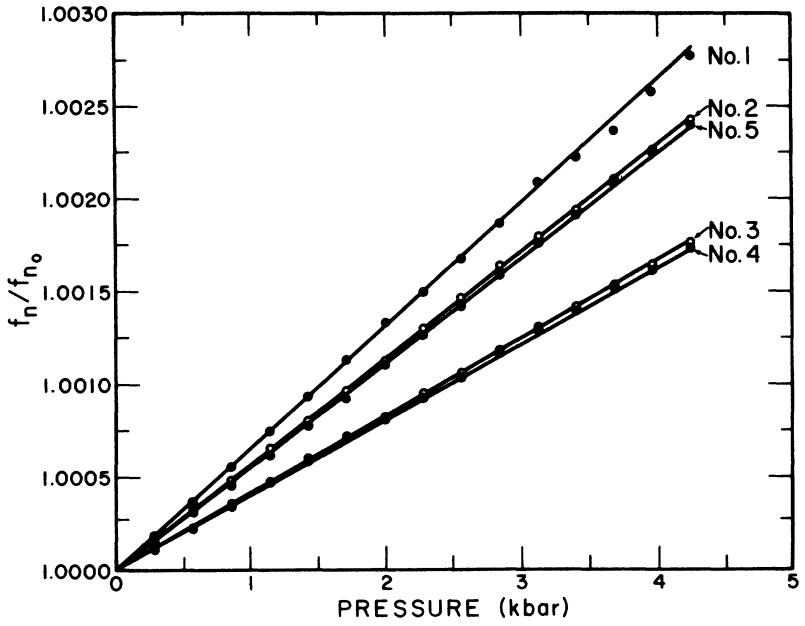

FIG. 1. Frequency ratio (f_n/f_{n_0}) versus pressure for various propagation modes which are explained in Table I.

seen, f_n/f_{n_0} versus pressure data are linear within experimental error except for f_1/f_{1_0}, which gives the elastic constant C_{11}. Measurements on this mode were repeated several times with different transducers after lapping the specimen surface. A dip in the frequency-pressure data above 3 kbar was consistently present in each experiment, although details of the curvature differed due to experimental scatter and changing bond thickness. The data shown for this mode in Fig. 1 are from one representative experiment. Even though this behavior was not found for the other modes, it is believed real because of its reproducibility, and not due to experimental error.

The least-squares-fit linear equations of (f_n/f_{n_0}) versus pressure (P, in kbar) are:

$$f_1/f_{1_0} = 1.000\,00 + 0.652\,08\times10^{-6}\,P, \quad r = 0.999\,72,$$
$$f_2/f_{2_0} = 1.000\,00 + 0.571\,93\times10^{-6}\,P, \quad r = 0.999\,93,$$
$$f_3/f_{3_0} = 1.000\,00 + 0.416\,690\times10^{-6}\,P, \quad r = 0.999\,96,$$
$$f_4/f_{4_0} = 1.000\,00 + 0.409\,170\times10^{-6}\,P, \quad r = 0.999\,88,$$
$$f_5/f_{5_0} = 1.000\,00 + 0.567\,99\times10^{-6}\,P, \quad r = 0.999\,89,$$

where r is the coefficient of correlation between f_n and P.

A modification of Cook's method[10,11] which accounts for the change in path length of the specimen under pressure, was used in analyzing the f_n/f_{n_0} versus pressure data in order to calculate C_{ij} at pressure. The adiabatic-isothermal conversion for the compressibilities were carried out using the well-known relations. The values of the thermodynamic parameters used in the computations are: volumetric thermal expansion,[3] $\alpha_V = 19.0 \times 10^{-6}\,°K^{-1}$, specific heat,[12] $C_p = 6.14$ cal/mole °K, and Grüneisen parameter, $\gamma = \alpha_V K_s/\rho C_p = 2.39$, where K_s is the adiabatic bulk modulus (adopted value of K_s is 3652 kbar). Table III shows the coefficients of compressibility and thermal expansion. The calculated values of C_{ij} versus pressure are shown in Fig. 2. Listed in Table IV are the values of dC_{ij}/dP obtained from the least-squares analysis of the data assuming linear relationship; the estimated uncertainties in dC_{ij}/dP include all experimental errors. The two values of dC_{44}/dP (calculated from the two modes 3 and 3A, Table I) agree to within 0.1% (1.489 vs 1.490, Table IV).

B. Isotropic elastic parameters

Isotropic values of various elastic parameters and their initial pressure derivatives calculated from the single-crystal data using the Voigt-Reuss-Hill approximation[13] are listed in Table V. In us-

TABLE III. Measured linear compressibilities and the thermal expansivity data (Ref. 3).

Coefficient	Value
$\beta_{\parallel}^{S}$	0.091995 ± 0.00131 Mbar^{-1}
$\beta_{\perp}^{S}$	0.090906 ± 0.00079 Mbar^{-1}
$\beta_{\parallel}^{T}$	0.092963 ± 0.00131 Mbar^{-1}
$\beta_{\perp}^{T}$	0.092279 ± 0.00079 Mbar^{-1}
$\alpha_{\parallel}$	$(4.96 \pm 0.07\times10^{-6})\,°C^{-1}$
$\alpha_{\perp}$	$(7.03 \pm 0.10\times10^{-6})\,°C^{-1}$

ing Overton's formula[14] for calculating dK_T/dP from dK_s/dP, $d\alpha/dT$ was assumed to be zero, and the value for dK_s/dT (−0.231 kbar/°K) was estimated from the data of Fisher and Dever.[2] The estimated errors in dK_s/dP and dK_T/dP (Table V) are based on all the uncertainties that are involved in the C_{ij} and dC_{ij}/dP measurements. Figure 3 presents the relations of density, adiabatic bulk modulus, shear modulus, and Poisson's ratio versus pressure.

IV. DISCUSSION OF RESULTS

A. K'_T and the Birch-Murnaghan equation

The pressure-volume data for a solid can be used for calculating its bulk modulus, K_T, and the initial pressure derivative, $K'_T = (\partial K_T/\partial P)_{P=0}$, through the Birch-Murnaghan equation of state,

$$P = \tfrac{3}{2}K_T\{(V_0/V)^{7/3} - (V_0/V)^{5/3}\}\{1 - \xi[(V_0/V)^{2/3} - 1]\}, \quad (1)$$

where P is pressure, V and V_0 are volumes at P and $P=0$, respectively, and $\xi = 3(4 - K'_T)/4$. Using Eq. (1), Liu *et al.*[3] have computed from the least-squares analysis of their x-ray data, the values of K_T and ξ as 3.50 ± 0.15 Mbar and 0.8 ± 1.0, respectively. By assuming K'_T to be 4.0 (i.e., $\xi = 0$), they obtained $K_T = 3.36 \pm 0.15$ Mbar. Their data and the two solutions are shown in Fig. 4. The value of K'_T derived from ξ is 2.93 ± 1.0; this value seems quite low. The relation of V/V_0 versus pressure, using the ultrasonic K_T and K'_T values (3.587 Mbar, and 5.43, respectively) in Eq. (1), is shown in Fig. 4. Also shown is the 20 °C isotherm established through the shock-wave data.[6] Comparisons among the three kinds of data (x-ray, ultrasonic, and shock wave) show closer agreement between the latter two than between the former two. The difference between the V/V_0 values at 200 kbar, based on the x-ray and ultrasonic data, is only about 0.7%, yet the values of K'_T deduced from the two methods vary by almost a factor of 2. That is, the parameter V/V_0 is not very sensitive to K'_T when K_T is so large—an inherent feature of the Birch-Murnaghan and similar equations of state. Hence, in view of the large K_T value for Re as well as the scatter in the x-ray data, there will, perforce, be large uncertainties in the K'_T values derived from the x-ray data; the differences between the K'_T values computed from the x-ray and ultrasonic data in the present case is probably related to some systematic errors in the former.

Bridgman's compressibility measurements on Re [15] are expressed in the relation $\Delta V/V_0 = -aP + bP^2$, in which a and b are constant quantities and P is pressure given in terms of kg/cm^2 (our discussion here will also be in these units). The quantity a is related to the isothermal bulk modulus, $a = (K_T)^{-1}$, and b is related to K'_T, $b = (K'_T + 1)/2\,K_T^2$.

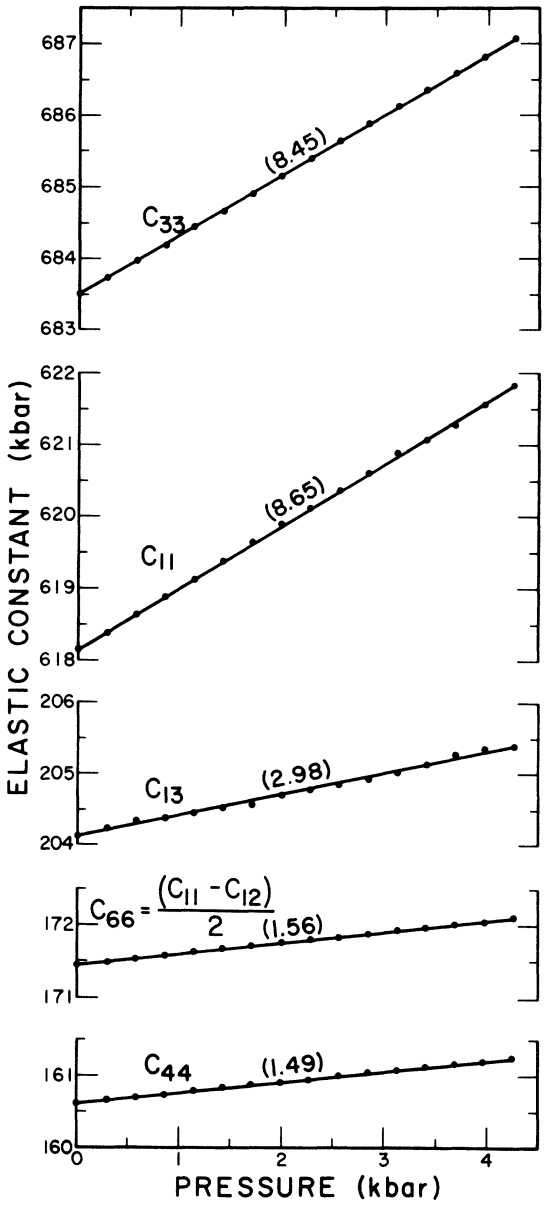

FIG. 2. C_{ij} versus pressure. The pressure derivatives are given in parentheses.

The value of b estimated from Bridgman's compression data to 30 kbar is 2.64×10^{-7} cm^2/kg,[15] which is comparable to our value of 2.72×10^{-7} cm^2/kg calculated from the foregoing formulation.

B. Relation of K'_T to ionic repulsion

The measured values of K'_T for various oxides and silicates lie in the range 4–6.8; K'_T is not commonly found to be significantly less than 4. In fact Anderson's[16] lower limit, in so far as the stability of an ionic cubic lattice is concerned, is 3.5.

TABLE IV. Pressure derivatives of elastic constants of Re at 25 °C.

Elastic constant C_{ij}	$\frac{dC_{ij}}{dP}$
C_{11}	8.65 ± 0.15
C_{33}	8.45 ± 0.14
C_{44}	1.49 ± 0.02
C_{44A}	1.49 ± 0.02
C_{66}	1.56 ± 0.03
C_{12}	5.52 ± 0.20
C_{13}	2.98 ± 0.29

For metals, the lowest reported K_T' values are in the neighborhood of 3.2–3.3, reported for the heavy rare earths (Gd, Dy, and Er),[17] and of 3.60 for Na.[18]

For metals, the value of K_T' is related to the Fermi energy of the free electrons and its dependence on volume, and the repulsive interaction between neighboring ion cores, which is due to the overlap or exchange energies. The former is a long-range contribution that dominates both K_T and K_T' when r_0, the equilibrium ionic separation, is relatively large, as in the alkali and rare-earth metals. The latter is a short-range interaction which is closely related to interatomic separation r of the nearest-neighbor atoms. The relative importance of the long- and short-range contributions to K_T and K_T', as well as to the shear moduli and their pressure derivatives, should then be closely related to atomic volume Ω. For large Ω the Fermi contribution should dominate, and if we assume a free-electron-gas model for K_F, the bulk modulus of the electron gas,

$$K_F = \frac{2}{3}\frac{E_F}{\Omega} Z^*, \tag{2}$$

then

$$K_F' = \frac{dK_F}{dP} = \frac{5}{3}\frac{K_F}{K_T} = \frac{E_F}{K_T\Omega}\frac{10}{9} Z^*, \tag{3}$$

where E_F is the Fermi energy, and Z^* is the effective valence, i.e., the number of free electrons per atom. As Ω decreases, the contribution from the repulsion increases. Assuming a Born-Mayer potential for this contribution, we can express the repulsive energy per bond, W, as:

$$W(r) = A \exp[-B(r/r_0 - 1)], \tag{4}$$

where A and B are material parameters, A having units of energy, and B, sometimes called "hardness" constant, is dimensionless. At $r = r_0$, we have $W(r) = A$. By differentiating Eq. (4), with respect to r, we get

$$\frac{dW}{dr} = W' = -\frac{B}{r_0} W, \tag{5}$$

Again,

$$W'' = \frac{B^2}{r_0^2} W \tag{6}$$

and

$$W''' = -\frac{B^3}{r_0^3} W. \tag{7}$$

Fuchs[19] obtained an expression for the short-range contribution to the bulk modulus, K_{SR}, for an fcc structure

$$\Omega K_{SR} = \tfrac{2}{3} r^2 W'', \tag{8}$$

by considering a nearest-neighbor model, with

TABLE V. Isotropic values of elastic parameters of Re at 25 °C and their initial pressure derivatives.

Elastic parameter, X	Value	$\frac{dX}{dP}$
Density, ρ	21.024 g/cm^3	5.82 (g/cm^3 Mbar)
Compressional-wave velocity, v_p	5.359 km/sec	2.716×10^{-3} (km/sec kbar)
Shear-wave velocity, v_s	2.917 km/sec	1.059×10^{-3} (km/sec kbar)
Adiabatic bulk modulus, K_s	3652 ± 15 kbar	5.41 ± 0.35
Isothermal bulk modulus, K_T	3603 ± 15 kbar	5.43 ± 0.35
Shear modulus, μ	1789 ± 9 kbar	1.80 ± 0.15
Poisson's ratio, σ	0.2894	0.086×10^{-3} kbar^{-1}
Debye temperature, Θ_D	395.06 °K	0.185 (°K/kbar)

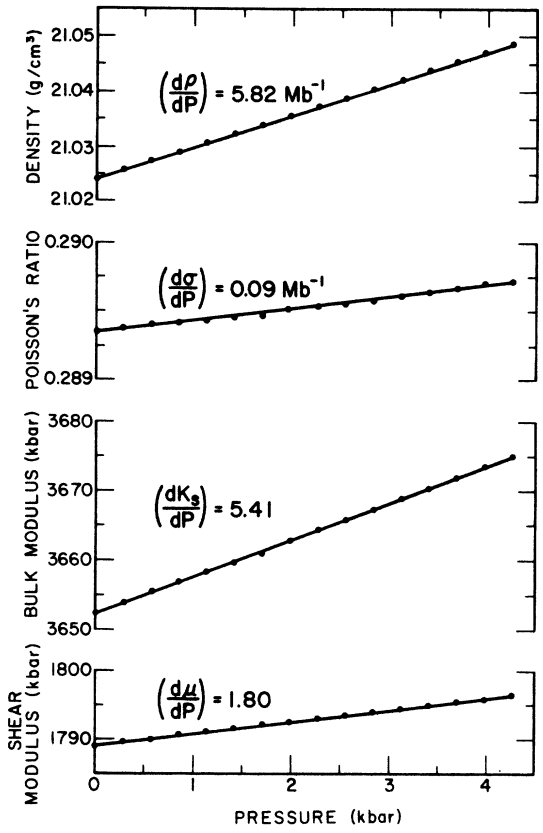

FIG. 3. Pressure dependence of density, Poisson's ratio and bulk and shear moduli. The pressure derivatives are given in parentheses.

central forces only between an atom and its twelve nearest neighbors. Since the Re structure has a c/a ratio very near to ideal closest packing with a coordination number of 12, and since the c/a ratio remains unchanged under initial hydrostatic pressure, i.e., $\beta_{\parallel}^{T} = \beta_{\perp}^{T}$ within the probable error of computing the compressibilities from the measured C_{ij}, we can reasonably assume that Eq. (8) holds for the short-range contribution to the bulk modulus, K_{SR} for Re. Differentiating Eq. (8) and using Eqs. (6) and (7) for W'' and W''', we have [since $W(r) = A$ at $r = r_0$]

$$\Omega \frac{dK_{SR}}{d\ln r} = \tfrac{2}{3}(r^3 W''' - r^2 W'') = -\tfrac{2}{3}B^2 A(B+1). \quad (9)$$

Further, since

$$\Omega \frac{dM}{d\ln r} = -3\Omega K_T \frac{dM}{dP}\ , \quad (10)$$

where M is any modulus and

$$\tfrac{2}{3}B^2 A = \Omega K_{SR}\,, \quad (11)$$

we obtain

$$K'_{SR} = \frac{dK_{SR}}{dP} = \frac{K_{SR}}{3K_T}(B+1). \quad (12)$$

Combining Eqs. (3) and (12), we get the following model equation for the experimental value of K'_T:

$$K'_T = K'_F + K'_{SR} = (1/K_T)[\tfrac{5}{3}K_F + \tfrac{1}{3}(B+1)K_{SR}]$$
$$= (1/9\Omega K_T)\,[2B^2 A(B+1) + 10\,E_F Z^*\,]. \quad (13)$$

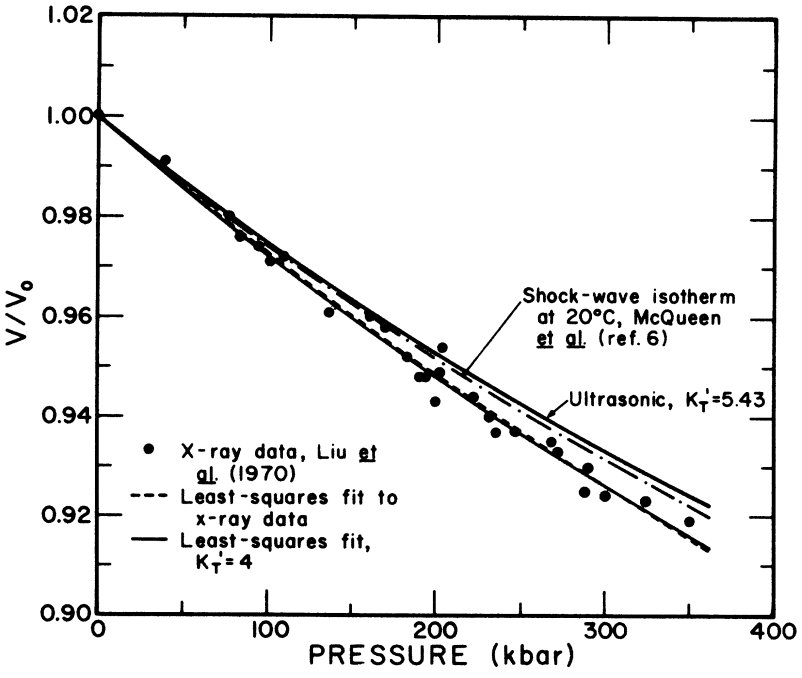

FIG. 4. V/V_0 versus pressure. Comparison of the x-ray, shock-wave, and ultrasonic results is shown.

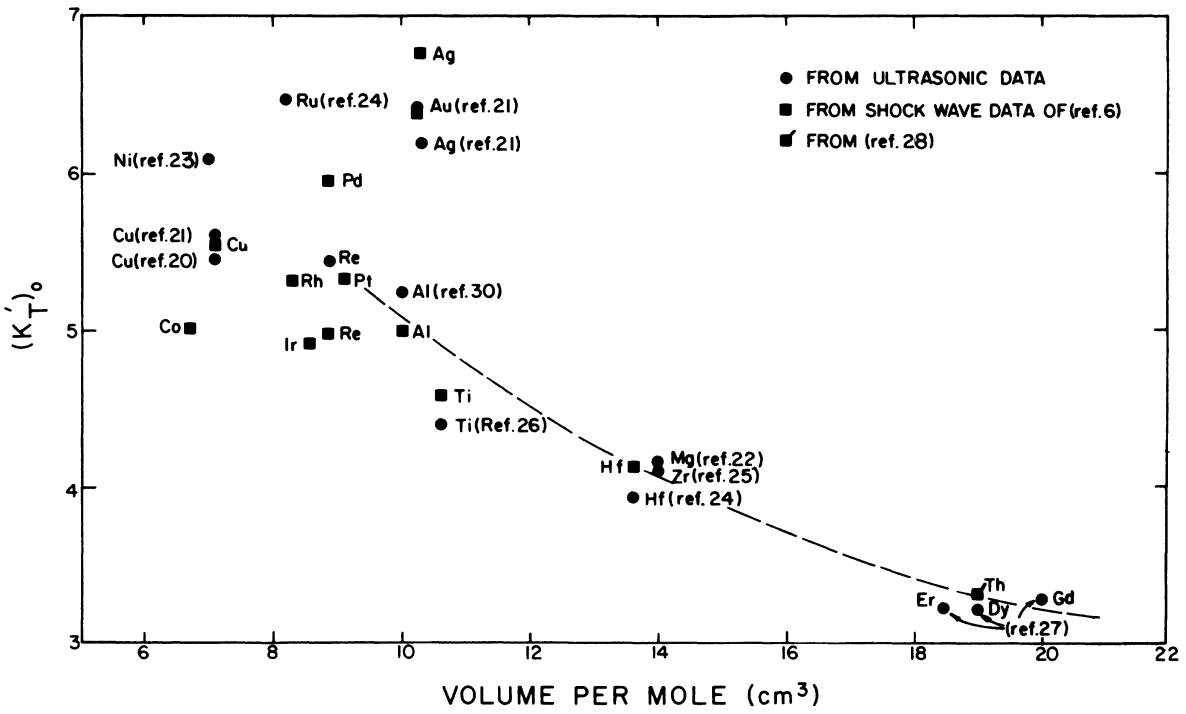

FIG. 5. K'_S versus atomic volume for several hcp, bcc, and fcc metals. Data for Hf and Ru are from our unpublished results.

This equation then serves, at least qualitatively, to relate K'_T (or K'_S, since $K'_T \approx K'_S$) to the atomic volume Ω of the metal at ambient pressure and thus to estimate whether a measured value of K'_T (or K'_S) is a reasonable one in relation to K'_T (or K'_S) of other metals. In Fig. 5 we have plotted the experimental K'_T (or K'_S) values from ultrasonic data versus molar volume for a number of close-packed metals of the hcp and fcc crystal structures.

The ultrasonic K'_T values are augmented by values of K'_T determined from fitting the pressure-volume data derived from shock-wave experiments[6] to Eq. (1). The average values of K'_T for each element as derived from the shock-wave data are noted in Fig. 5 by the squares, in contrast to the circles which represent ultrasonic data. For those elements where both ultrasonic and shock-wave data exist, the K'_T values agree to within 10%, except for the relatively small K'_T for Ag and Au (4.11 and 5.21, respectively) given by the ultrasonic data of Hiki and Granato.[20] For Au the shock-wave data give a K'_T that is almost precisely the ultrasonic value of Daniels and Smith,[21] whereas for Ag the shock-wave K'_T value is about 10% greater than the Daniels and Smith value but 65% greater than the Hiki and Granato value. On the basis of the above comparison, it appears that the high values of K'_T for Ag and Au are more accurate and one may conclude that K'_T is equal to or greater than 5 for the noble metals, Cu, Ag, and Au, and for the close-packed transition metals with more than half-filled d electron shells. For the group-IV hcp metals K'_T decreases with increasing atomic volume and for the hcp rare earths, all of which have relatively large Ω values, K'_T remains relatively small (~ 3.2) but insensitive to Ω.

It is interesting to note that for Th, the one actinide fcc metal for which data exist, the K'_T and Ω values coincide with the rare-earth data.

The qualitative conclusion from Fig. 5 is that the Born-Mayer parameters A and B are of greater importance as Ω decreases below 18 cm^3 per mole. In the lower range of Ω the K'_T values are determined primarily by the short-range forces, whereas in the intermediate-Ω region the K'_T value is sensitive to the interatomic distances through the short-range contribution.

C. Evaluation of the Born-Mayer parameters

One of the interesting applications of K'_T (or K'_S) data is the evaluation of parameters A and B in Eq. (4). To do this, however, requires that the measured K_T and K'_T values be apportioned between the Fermi and repulsive terms so that B can be extracted from Eq. (12) and A from Eq. (11). This separation is unfortunately not a well-defined process in the present case because of the assumption in Eqs. (2) and (3), namely, the free electron gas

with a spherical Fermi surface. Because the electron band structure and the actual Fermi surface are evidently considerably more complex than for a free-electron gas, K_F and K'_F are subject to considerable doubt. It appears that some information regarding the relative contributions to K_T and K'_T can be obtained by deriving parameters A and B in Eq. (4) from two models: model (1), in which we assume full electronic contributions based on calculated E_F and Z^* values; and model (2), in which we assume that the measured K_T and K'_T values are derived entirely from the short-range forces.

To evaluate Z^* we have used the value of 0.825 Ry for E_F obtained from augmented-plane-wave (APW) calculations,[29] and assumed a spherical Fermi surface containing $Z^* = 2.49$ electrons per atom for Re, and $K_F = 2.017 \times 10^{12}$ dyn/cm^2. Assuming $K_{SR} = K_T - K_F$ for model (1), and knowing K_T (3720 kbar at 4 °K), we get $K_{SR} = 1703$ kbar. Then $K'_{SR} = K'_T - K'_F$, and thus we obtain

$$K'_{SR} = (5.43 - 0.93) = 4.5 ,$$

and from Eq. (12), we have

$$B + 1 = 4.5(3K_T/K_{SR}) = 28.54 ,$$

or $B = 27.54$. Using this value in Eq. (11) we obtain $A = 0.03$ eV at $r = r_0$. For the second model, where K_F and K'_F are assumed not to contribute significantly to K_T and K'_T, we obtain $A = 0.22$ eV and $B = 15.3$. The values of the parameters and results are summarized in Table VI.

As a basis for deciding which of the two models is more reasonable, we have carried out similar calculations for Cu and Au, based on the values of K_T at 300 °K, and K'_T values of Daniels and Smith.[21] The results and other previous data[29] are shown in Table VI. As seen, model (1) gives values of B and A for Cu which are similar to those calculated for Re, but are extremely high and low, respectively, when compared to those obtained by other means.[30-32] The values for Cu based on model (2) are more consistent with the Mann and Seeger[30] values; the value of B for Cu is the same as that for Re, since in the two cases the K'_T values are identical within the error of measurement. For Au, the results of the two models are not as widely different as for Cu or Re. Nevertheless, the B and A values for model (2) are very close to those derived by Thompson[31] from neutron-channeling experiments. We thus conclude that the Fermi contribution to the K_T and K'_T of Re is probably considerably smaller than that derived from the free electron spherical Fermi surface, and that model (2) considered above applies well to Re.

Although the values of B are very similar for the three metals (Table VI), the A value for Re, based on model (2), is considerably greater than

TABLE VI. Comparison of the values of the Born-Mayer parameters calculated from models (1) and (2) with those reported by other investigators.

Metal	Model and/or reference	K_{SR} (Mbar)	K'_T	K'_{SR}	B	A (eV)
Re	Model (1)	1.703	5.43	4.5	27.5	0.03
	Model (2)	3.72	5.43	5.43	15.3	0.22
Cu	Model (1)	0.79	5.60	4.86	23.6	0.026
	Model (2)	1.42	5.60	5.60	15.8	0.06
Cu	Mann and Seeger (Model a) (Ref. 30)				13.6–26.9	0.077–0.011
Cu	Mann and Seeger (Model b) (Ref. 30)				11.8–12.6	0.108–0.075
Cu	Gibson *et al.* (Ref. 32)				10.34–16.97	0.1004–0.0392
Au	Model (1)	1.31	6.43	6.01	21.8	0.04
	Model (2)	1.66	6.43	6.43	18.3	0.08
Au	Mann and Seeger (Model a) (Ref. 30)				16.3–30.5	0.040–0.008
	Mann and Seeger (Model b) (Ref. 30)				11.6–12.0	0.150–0.128
Au	Thompson (Ref. 31)				14.4	0.11

that for Cu and Au. This is consistent with the relative cohesive energies calculated for the three metals, where the ratios for Re, Au, and Cu are 8.1, 3.78, and 3.50 eV/per atom, respectively.[33]

D. Contributions to the shear moduli

The volume dependence of the shear moduli have a major influence on the mode-averaged Grüneisen gamma. In the present case, there are three contributions to the shear moduli that should be considered. These are: (i) the short-range repulsion between ion cores; (ii) the purely electrostatic term that is derived from the force between positive ions in a uniform electron distribution; and (iii) the Fermi-energy term that arises in polyvalent metals because of the proximity of the Fermi surface to the Brillouin-zone boundaries. The electrostatic contributions to C_{44}, C_{66}, and $C_H = \frac{1}{6}(C_{11}+C_{12}+2C_{33}-4C_{13})$ shear moduli, denoted by C_s^e, and their pressure derivatives, can be approximated from Fuch's formulas[19] and the Coulomb sum factors calculated for hcp metals by Cousins.[34] Since the linear compressibilities $\beta_\parallel$ and $\beta_\perp$ are essentially equal in Re (Table V), we are not concerned here with the change in the c/a ratio under hydrostatic pressure. The electrostatic-contribution terms therefore are

$$C_s^e = -M_s Z^{*2}/\Omega_0 r_0 , \tag{14}$$

$$\pi_s^e = \frac{d\ln C_s^e}{d\ln\Omega} = -\frac{4}{3} , \tag{15}$$

where C_s represents the modulus (C_{44}, C_{66}, or C_H), M_s is the electronic charge times the Coulomb sum factor,[34] and r_0 is the interatomic distance in the basal plane. The observed values of π_s are given in Table VII. The values of π_{44}, π_{66}, and π_H are considerably larger than $-\frac{4}{3}$, and indicate that the contributions from the short-range and/or the Fermi terms are of major importance. To obtain an estimate of the relative importance of the electrostatic, short-range, and Fermi contributions, it is convenient to express the effects of pressure on C_S in the form of some function of the interatomic distance r. We have then the following expressions:

$$-3\Omega_0 K_T \frac{dC_s}{dP} = \Omega_0 \frac{dC_s}{d\ln r} = \frac{\Omega_0}{d\ln r}(dC_s^e + dC_s^{SR} + dC_s^F) , \tag{16}$$

where the electrostatic term $\Omega_0 dC_s^e/d\ln r$ is given as

$$\frac{\Omega_0 dC_s^e}{d\ln r} = -4\Omega_0 C_s^e . \tag{17}$$

On the assumption that the effective valence of the Re ion is 2.49, as calculated from E_F on the basis of a spherical Fermi surface, the C_s^e values from Eq. (14) can then be used to derive quantitative data for the short-range and Fermi contributions:

$$\frac{\Omega_0}{d\ln r}(dC_s - dC_s^e) = \frac{\Omega_0}{d\ln r}(dC_s^{SR} + dC_s^F) . \tag{18}$$

The values of these quantities are also given in Table VII.

The results shown in Table VII indicate that the electrostatic contributions to the shear moduli are indeed minor and that at least 75% of the pressure derivative of each shear modulus is due to the short range and/or Fermi energy changes with distortion. The results also indicate that the nonelectrostatic contributions to dC_H/dp are about twice those for dC_{44}/dP and dC_{66}/dP.

As background to the Fermi-energy contribution to the shear moduli of Re, it should be noted that the variation of the superconducting transition temperature with hydrostatic pressure is anomalous in that T_c is a minimum at ~7 kbar and dT_c/dP changes rather significantly at $P>2$ kbar.[4] This change in dT_c/dP has been interpreted as an abrupt change in the Fermi-surface topology at some pressure <7 kbar.[5]

If the Fermi energy is a major factor contributing to the shear moduli or the bulk modulus, we should find some nonlinearity in the relationship between these moduli and the pressure. As can be seen in Figs. 2 and 3, C_{44}, C_{66}, and K_T are quite linear with pressure, suggesting that the major contributions to K_T, C_{44}, C_{66} and their derivatives in Re come from the short-range ion-core repulsive force and not from the Fermi-surface energy.

On the other hand, C_{11} (Fig. 2) and C_H (Fig. 6) do show nonlinearity. C_H is calculated from $C_H = \frac{1}{6}(C_{11}+C_{12}+2C_{33}-4C_{13})$, and since C_{12} and C_{13} are also calculated quantities which depend on C_{11}, it is clear that the behavior of C_H is directly related to that of C_{11}. As discussed earlier in Sec. IIIA, the nonlinearity of C_{11}, and hence that of C_H is believed to be real, and not due to random experimental errors. As seen in Fig. 6, dC_H/dP is constant to about 3 kbar, but undergoes a systematic change between 3 and 4 kbar when dT_c/dP also

TABLE VII. Observed values of π_s (dimensionless), and calculated values of $\Omega dC_s/d\ln r$ for C_s^e and $C_s^{SR}+C_s^F$ in units of 10^{-12} erg.

	Modulus C_s		
Parameter	C_{11}	C_{66}	C_H
π_s	-3.34 ± 0.02	-3.28 ± 0.02	-4.78 ± 0.10
$\frac{\Omega dC_s^e}{d\ln r}$	-30.3	-48.9	-69.3
$\frac{\Omega(dC_s^{SR}+dC_s^F)}{d\ln r}$	-206.5	-199.0	-437.6

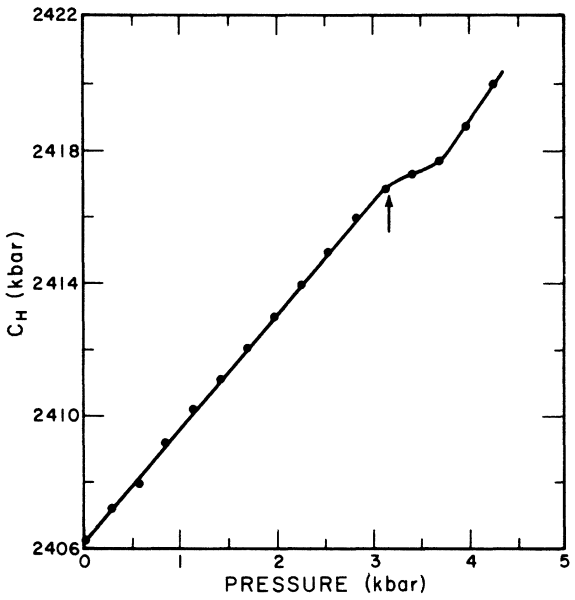

FIG. 6. $\frac{1}{6}C_H = (C_{11} + C_{12} + 2C_{33} - 4C_{13})$ versus pressure. Note the deviation in slope at pressure > 3 kbar.

becomes nonlinear. Since C_H denotes the resistance to change in c/a ratio at constant volume, the decrease in C_H from a constant dC_H/dP indicates that some sort of Fermi-surface–zone-boundary overlap occurs in the range of 3–4 kbar.

E. Grüneisen constant

The Grüneisen mode gamma γ_H calculated from the dC_{ij}/dP using Gerlich's procedure,[35] as adapted in another paper,[26] is 1.83 as compared to 2.39 for the thermal Grüneisen parameter at 300 °K calculated from the thermodynamic relation,

$$\gamma_{th} = \alpha_V K_s / \rho C_p ,$$

Gschneidner's[12] value for γ_{th}, based on an earlier measurement of α_V, is still higher: 2.66.

The reason for the discrepancy between γ_H and γ_{th} (1.83 vs 2.39) is not clear, but we do not expect it to be associated with the $\Delta(c/a)$ effect[25,26] for two reasons: (i) the two compressibilities $\beta_{\parallel}$ and $\beta_{\perp}$ are equal for Re; and (ii) the $\Delta(c/a)$ effect is evidently a significant factor when the electrostatic contributions to the shear moduli are relatively important.[34] Hence, in the present case, where the interatomic repulsion seems to be the prime contribution, the c/a ratio should not have a major effect on the calculation of γ_H. There are several sources of possible error here, as well as the real effect of the pressure derivatives of the optic modes which are not included in the averaging of the acoustic-mode γ's. The mode γ's associated with the optical vibrations may be considerably larger than the acoustic-mode γ's.

F. Summary

The elastic constants C_{ij} of single-crystal Re have been measured to ~4.2 kbar. The value of $K'_T = (\partial K_T/\partial P)_{P=0}$ is 5.43 ± 0.35, which is appreciably larger than the x-ray compression-data value of 2.93 ± 1.33, but is consistent with the shock-wave data and with the K'_T-atomic-volume relationship found for various metals belonging to the hcp and fcc crystal structures. The correlation indicates that K'_T is a very useful parameter for determining the relative importance of long- and short-range forces to the elastic properties of metals.

From the evaluation of the Born-Mayer potentials, it is concluded that the short-range repulsive interatomic forces are the dominant contributions to K'_T in Re, as is the case for the noble metals Cu, Au, and Ag. A similar conclusion is indicated for the shear moduli, where the volume derivatives are far in excess of that expected from the long-range electrostatic forces.

The pressure dependence of C_{ij} is linear except in the cases of C_{11} and $C_H = \frac{1}{6}(C_{11} + C_{12} + 2C_{33} - 4C_{13})$ moduli which show nonlinear behavior at ~3.3 kbar. This effect correlates with the anomalous pressure dependence of superconducting temperature T_c to approximately the same pressure, and reflects the abrupt change in the Fermi-energy surface at that pressure.

ACKNOWLEDGMENTS

The skillful assistance of John Balogh in maintaining the high-pressure equipment is acknowledged. This research was supported by National Science Foundation Grant No. GK-29750 to the University of Hawaii. Work at the Argonne National Laboratory was supported by the Physical Research Division, U.S. Atomic Energy Commission. We thank Lin-Gun Liu and William A. Bassett for helpful comments on the paper.

*Research supported by National Science Foundation Grant No. GK-29750.

[1]M. L. Shepard and J. F. Smith, J. Appl. Phys. 36, 1447 (1965).

[2]E. S. Fisher and D. Dever, Trans. Metall. Soc. AIME 239, 48 (1967).

[3]L. Liu, T. Takahashi, and W. A. Bassett, J. Phys. Chem. Solids 31, 1345 (1970).

[4]C. W. Chu, T. F. Smith, and W. E. Gardner, Phys. Rev. Lett. 20, 198 (1968).

[5]C. W. Chu, T. F. Smith, and W. E. Gardner, Phys. Rev. B 1, 214 (1970).

[6]R. G. McQueen, S. P. Marsh, J. W. Taylor, J. N. Fritz, and W. J. Carter, in *High Velocity Impact Phenomena*, edited by R. Kinslow (Academic, New York, 1970), p. 293.

[7]H. J. McSkimin, J. Acoust. Soc. Am. 33, 12 (1961).
[8]M. H. Manghnani, E. S. Fisher, and W. S. Brower, Jr., J. Phys. Chem. Solids 33, 2149 (1972).
[9]M. H. Manghnani, J. Am. Ceram. Soc. 55, 360 (1972).
[10]R. K. Cook, J. Acoust. Soc. Am. 29, 445 (1957).
[11]M. H. Manghnani, J. Geophys. Res. 74, 4317 (1969).
[12]K. A. Gschneidner, Solids State Phys. 16, 275 (1964).
[13]O. L. Anderson, J. Phys. Chem. Solids 27, 547 (1966).
[14]W. C. Overton, Jr., J. Chem. Phys. 37, 116 (1962).
[15]P. W. Bridgman, Proc. Am. Acad. Arts Sci. 84, 111 (1955).
[16]O. L. Anderson, in *The Nature of the Solid Earth*, edited by E. S. Robertson, L. Knopoff, and J. F. Hays (McGraw-Hill, New York, 1971), P. 575.
[17]E. S. Fisher, M. H. Manghnani, and R. Kikuta, J. Phys. Chem. Solids 34, 681 (1973).
[18]W. D. Daniels, Phys. Rev. 119, 1246 (1960).
[19]K. Fuchs, Proc. Roy. Soc. A 153, 622 (1936); Proc. Roy. Soc. A 157, 444 (1936).
[20]Y. Hiki and A. V. Granato, Phys. Rev. 144, 411 (1966).
[21]W. B. Daniels and C. S. Smith, Phys. Rev. 111, 713 (1958).
[22]R. E. Schmunk and C. S. Smith, J. Phys. Chem. Solids 9, 100 (1959).
[23]V. P. N. Sarma and P. J. Reddy, Philos. Mag. 27, 769 (1973).
[24]M. Manghnani (unpublished).
[25]E. S. Fisher, M. H. Manghnani, and T. J. Sokolowski, J. Appl. Phys. 41, 2991 (1970).
[26]E. S. Fisher and M. H. Manghnani, J. Phys. Chem. Solids 32, 657 (1971).
[27]E. S. Fisher, M. H. Manghnani, and R. K. Kikuta, J. Phys. Chem. Solids 34, 687 (1973).
[28]D. J. Pastine and D. Piacesi, J. Phys. Chem. Solids 27, 1783 (1966).
[29]L. F. Mattheiss, Phys. Rev. 151, 450 (1966).
[30]E. Mann and A. Seeger, J. Phys. Chem. Solids 12, 314 (1960).
[31]M. W. Thompson (unpublished).
[32]J. B. Gibson, A. N. Goland, M. Milgram, and G. H. Vineyard, Phys. Rev. 120, 1229 (1960).
[33]C. Kittel, *Introduction to Solid State Physics*, 4th ed. (Wiley, New York, 1971).
[34]C. S. G. Cousins, J. Phys. C 1, 478 (1968).
[35]D. Gerlich, J. Phys. Chem. Solids 30, 1638 (1969).